JOURNAL OF GEOPHYSICAL RESEARCH, VOL. 105, NO. B8, PAGES 19,393–19,403, AUGUST 10, 2000

Size dependence of hysteresis properties of small pseudo-single-domain grains

Andrew J. Newell[1] and Ronald T. Merrill
Geophysics Program, University of Washington, Seattle

Abstract. The Day plot (M_{rs}/M_s versus H_{cr}/H_c) is widely used by paleomagnetists to estimate the size of ferromagnetic grains and classify them as single-domain (SD), pseudo-single-domain (PSD,) or multidomain (MD). How reliable is this plot? To find out, a numerical micromagnetic model is used to calculate hysteresis loops as a function of grain size for two grain shapes (cube and cuboid with $X = 1.5Y = 1.4Z$). Magnetocrystalline anisotropy is ignored. The average M_{rs}/M_s is calculated for a collection of randomly oriented grains: In the elongated grain it drops from 0.4 to 0.06 over a negligible size range, almost missing the usual PSD range altogether. Other hysteresis parameters, H_c, H_{cr}, and χ_0, can only be calculated for a grain at a time. This is done for two magnetic field directions (close to the longest axis and close to the shortest axis). The single-grain values of H_{cr}/H_c depend strongly on field direction, but it is clear that the average jumps rapidly from SD to MD values. There are large, rapid fluctuations in H_{cr} and χ_0 associated with changes in remanent states. However, these fluctuations may not be apparent when averaged over a broad size range. This may explain why H_{cr} and χ_0 depend weakly on grain size in real samples. In the size range studied ($L \leq 0.25\,\mu$m), hysteresis parameters do not represent a typical grain size. Instead, they depend strongly on the size distribution.

1. Introduction

The complex hysteretic response of a ferromagnet to a magnetic field is commonly represented by four parameters: the normalized saturation remanence M_{rs}/M_s, the coercivity H_c, the coercivity of remanence H_{cr}, and the initial susceptibility χ_0. In applications such as paleomagnetism and environmental magnetism these parameters are used to infer the composition, grain size, and concentration of the magnetic minerals [*Thompson and Oldfield*, 1986; *Verosub and Roberts*, 1995]. The most reliable information on grain size dependence comes from measurements on synthetic samples with known sizes. For magnetite [*Heider et al.*, 1987] and many other minerals [*Dunlop and Özdemir*, 1997], M_{rs} decreases roughly as $L^{-0.7}$ and H_c as $L^{-0.4-0.5}$. By contrast, χ_0 and H_{cr} vary little with grain size [*Heider et al.*, 1996]. However, there is a large scatter about these trends. Most rock magnetists attribute this scatter to differences in defect density, but it could also be caused by differences in size distribution. Even samples with grown magnetite crystals typically have size ranges of an order of magnitude. Are hysteresis parameters accurate indicators of the mean grain size of a sample, or are they also sensitive to the distribution about the mean?

Paleomagnetists often plot M_{rs}/M_s against H_{cr}/H_c. *Day et al.* [1977] recommended this plot because a suite of titanomagnetites with varying titanium composition and grain size all fell roughly on the same curve. They argued that this indicated the different materials all underwent the same sequence of changes in domain structure, so their plot was a universal indicator of domain structure. Following their example, the plot is usually divided into regions: single-domain (SD) for $M_{rs}/M_s > 0.5$ and $H_{cr}/H_c < 1.5$, multidomain (MD) for $M_{rs}/M_s < 0.05$ and $H_{cr}/H_c > 4$, and pseudo-single-domain (PSD) in between.

If M_{rs}/M_s and H_{cr}/H_c were always strongly correlated, there would be no need for both parameters. However, natural samples often do not lie on the same curve [*Jackson*, 1990; *Gee and Kent*, 1995; *Suk and Halgedahl*, 1996]. *Tauxe et al.* [1996] calculated hysteresis parameters for mixtures of superparamagnetic (SP) and SD grains and showed they could be almost anywhere within the PSD region on a Day plot, depending on the magnitude of the anisotropy and the grain size distribution. Thus we must ask: Can the Day plot, or the hysteresis parameters separately, even distinguish between SP/SD mixtures and larger grains?

Until we can constrain the grain size better in synthetic samples, we must address the above questions

[1]Now at Geological Sciences Department, University of California, Santa Barbara.

Paper number 2000JB900122.
0148-0227/00/2000JB900122$09.00

using theory. In section 2 we review previous hysteresis theories. In section 3 we describe how we use the micromagnetic model of *Newell and Merrill* [this issue] to calculate hysteresis parameters. In section 4 we present our calculations of M_{rs}, H_c, H_{cr}, and χ_0, and we construct the first synthetic Day plot for PSD grains.

2. Previous Work

In SD grains, changes in magnetization occur by uniform rotation, and they can be predicted by a simple theory [*Stoner and Wohlfarth*, 1947]. We display those predictions in Table 1 for pure shape (magnetostatic) anisotropy. ΔN, the SD demagnetizing factor, decreases from 1/3 to 0 (SI units) as the aspect ratio increases from 1 to infinity. If uniaxial magnetocrystalline or magnetoelastic terms are added (for a review of these energy terms, see *Dunlop and Özdemir* [1997]), the only effect is to replace ΔN by another factor.

In MD grains the primary modes of change in magnetization are domain wall motion and domain transitions (creation or annihilation of domain walls). When a field is applied, it pushes the domain walls around, but spatial variations in the anisotropy (due to defects, for example) exert a frictional force opposing the motion of the walls. The domain pattern can be very complex [*Hubert and Schäfer*, 1998], and each energy term affects it differently.

MD hysteresis theories simplify the problem by assuming lamellar domains and ignoring domain transitions. The MD expressions in Table 1 are based on a further simplification called the internal field approximation [e.g., *Néel*, 1955; *Stacey*, 1963]. This approximation is an attempt to separate the effects of grain size and shape from the properties of the material. The total magnetic field is separated into two components: $H = H_i + N_{\mathrm{MD}}M$, where N_{MD} is a MD demagnetizing factor and H_i is called the intrinsic field. It is assumed that grain size and shape affect only N_{MD}, while H_i is determined by the material properties (including the defect structure). Two parameters represent the dependence of H_i on M: the intrinsic susceptibility $\chi_i \equiv dM/dH_i$ and the coercivity $H_c \equiv H_i(M = 0)$. The expressions in Table 1 show how the measured hysteresis parameters are determined by N_{MD}, χ_i, and H_c.

The MD theory only predicts some relations between hysteresis parameters. It does not actually predict hysteresis parameters (let alone a complete hysteresis curve) for a particular grain size and shape. It is generally expected that large grains are soft, with large χ_i and small H_c. As $\chi_i \to \infty$, $H_{cr}/H_c \to \infty$ and χ_0 approaches $1/N_{\mathrm{MD}}$ from below. As $H_c \to 0$, $M_{rs} \to 0$. If we wish to make more detailed predictions, we must solve the equations for wall pinning in a grain for which the size, shape, and defect structure are specified. In practice, the parameters H_i, H_c, and N_{MD} depend on all these factors, so they are not really independent [*Newell*, 1997].

A more fundamental problem with the MD theories is that they cannot account for transitions between domain states. Yet the creation or annihilation of domain walls is a major reorganization of magnetization, and it should have a large effect on the moment. Recent experiments combining hysteresis measurements with domain observations on single grains confirm that it does [*Halgedahl*, 1995].

A good theory for hysteresis in large grains should calculate hysteresis curves self-consistently and should be able to represent transitions between domain states. This is what micromagnetic theory [*Brown*, 1963] was designed to do. However, until recently, micromagnetic models were used mainly to calculate remanent states. With the exception of *Newell et al.* [1993b] and *Williams and Dunlop* [1995], the calculations were not tied to a particular process such as isothermal hysteresis or grain growth, so little could be said about when each remanent state occurred.

Previous authors have calculated susceptibilities using a lamellar micromagnetic model [*Enkin*, 1986] and a one-dimensional model of a cylinder [*Heider et al.*, 1996]. In the latter model the field is aligned with the long axis of the cylinder. When the magnetocrystalline easy axis is also aligned with the long axis, χ_0 increases as the grain size approaches the SD size range. It does not approach the SD value for this configuration, which is zero. *Heider et al.* [1996] do not comment on this. We will show that a similar effect occurs more generally and is related to nucleation.

3. Micromagnetic Model

Our methods are described in detail by *Newell and Merrill* [this issue]. They are similar to previous models [e.g., *Williams and Dunlop*, 1989; *Berkov et al.*, 1993]

Table 1. SD and MD Predictions for Hysteresis Parameters

	SD[a]	MD[b]
M_{rs}	$0.5M_s$	H_c/N_{MD}
χ_0	$2/(3\Delta N)$	$\chi_i/(1+\chi_i N_{\mathrm{MD}})$
H_c	$0.479\Delta N M_s$	H_c
H_{cr}	$1.09H_c$	$(1+\chi_i N_{\mathrm{MD}})\,H_c$

[a] *Stoner and Wohlfarth* [1947].
[b] *Stacey* [1963].

except that we have developed strategies to identify new stable states and avoid unstable ones. We simulate hysteresis cycles, starting with a field that is large enough to nearly saturate the magnetization. We pay special attention to points where states change stability (nucleation and jumps in magnetization). When more than one jump occurs in the main loop, we look for minor branches. To avoid unstable branches, we add a random perturbation before each step in the field.

We use a three-dimensional numerical model to solve the micromagnetic equations for cuboids with dimensions $X \times Y \times Z$. The grains are divided into $N \times M \times L$ cells, and within each cell the magnetization is approximated by a uniform magnetization. We have concentrated on two shapes, a cube and a cuboid with $X = 1.5Y = 1.4Z$. We define the grain size as the cube root of the volume $L = (XYZ)^{1/3}$. The only energy terms are the exchange energy and the magnetostatic energy, so there is a characteristic length scale $L_{ex} = (A/\mu_0 M_s^2)^{1/2}$. We use parameters suitable for magnetite, $A = 1.3\times10^{-11}\,\mathrm{J\,m^{-3}}$ and $M_s = 4.8\times10^{5}\,\mathrm{A\,m^{-1}}$, and we give lengths for magnetite grains, but the results can be scaled to other materials by keeping the ratio L/L_{ex} constant.

We do not include the effect of thermal fluctuations, which will reduce H_c and H_{cr} and will also start to reduce M_{rs} as the grain size approaches the threshold for superparamagnetism. We also leave out magnetocrystalline and magnetoelastic anisotropy. It may seem more realistic to include these terms, but it adds greatly to the complexity of the problem because there are many more possible states for any given field. As we will see in section 4, the changes in magnetization are sufficiently complex without magnetocrystalline anisotropy. In addition, the easy axes in natural samples are not necessarily along symmetry axes of the body, so a particular crystallographic orientation does not represent all grains. Finally, when the magnetocrystalline anisotropy is cubic (as in magnetite), it is generally weak and may not have a large effect on the moment. We will attempt to gauge its importance by comparing our calculations with some that include magnetocrystalline anisotropy in a particular orientation [*Williams and Dunlop*, 1995; *Fabian et al.*, 1996], but the interpretation will be complicated by questions of stability.

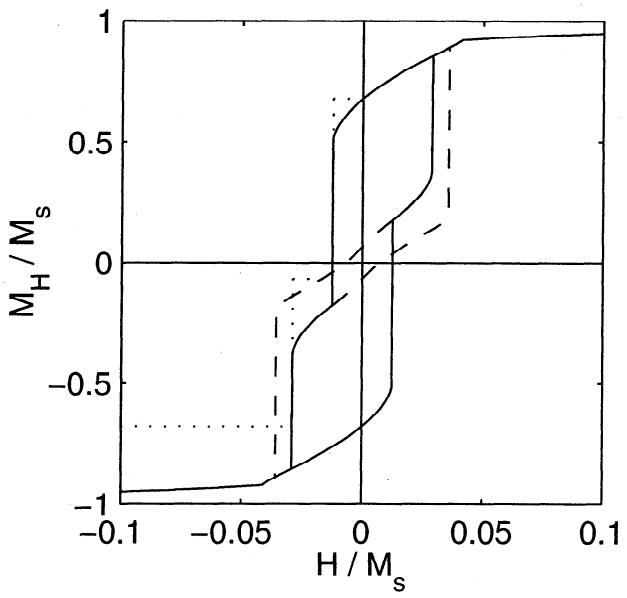

Figure 1. Illustration of the methods of calculating hysteresis parameters. For a triaxial cuboid with $L = 0.09\,\mu$m and $\mathbf{H} \parallel (8,4,1)$ the main loop is shown as solid curves and minor branches are shown by dashed curves. The saturation remanent state has a moment along the longest axis, while the remanent state on the minor branch has a moment along the shortest axis. The remanences and locations of jumps are used to construct the back field remanence curve (dotted curve).

Our goal is to calculate some of the important hysteresis parameters as a function of grain size. Our methods are illustrated in Figure 1. We call the component of magnetization in the direction of the field M_H. This plot has a main loop and a couple of minor branches. The corresponding remanent states have moments along the longest and shortest axes (section 4). In single grains, irreversible changes occur only at jumps in the hysteresis loop, so a back field remanence curve is composed of horizontal segments and vertical jumps, as shown. H_{cr} is the magnitude of the back field for which the remanence changes sign. M_{rs} and H_c are the positive intercepts of the main loop.

The initial susceptibility is usually measured for a demagnetized state. We will assume alternating field (AF) demagnetization. We can determine the AF demagnetized state by following the hysteresis curve around as the field changes. In Figure 1 this leads to a remanent state on a minor branch. We assume an equal number of up and down states, and we calculate $\chi_0 \approx \Delta M_H/\Delta H$ for $H = \pm 0.002 M_s$, where M_H is the component of magnetization in the direction of the field. (For magnetite, $0.002M_s \approx 1.2\,\mathrm{m\,T}$.) The hysteresis curve is linear in fields this small.

Finally, hysteresis properties for single grains depend strongly on the direction of the field. For example, in Figure 2 we show a hysteresis loop for the same grain size as in Figure 1 but with $\mathbf{H} \parallel (1,8,4)$. The $(8,4,1)$ direction has an angle of 27° with respect to the longest axis, while the $(1,8,4)$ direction has the same angle with respect to the shortest axis. In this article, we use those two directions to represent the dependence of hysteresis on field direction.

Newell and Merrill [1999] showed that most jumps occur at turning points defined by an approach of the slope $\chi(H) = dM_H/dH$ to infinity. When we find a turning point, it confirms that the jump is correctly located. Unfortunately, not all jumps are associated with turning points [*Iooss and Joseph*, 1990]. In our simulations, most jumps occurred at turning points when $\mathbf{H} \parallel (8,4,1)$, but when $\mathbf{H} \parallel (1,8,4)$, we could not always find a turning point (for example, $H \approx 0.18M_s$ in Figure 2). When we did not see a turning point, we did not know whether the program was missing the correct

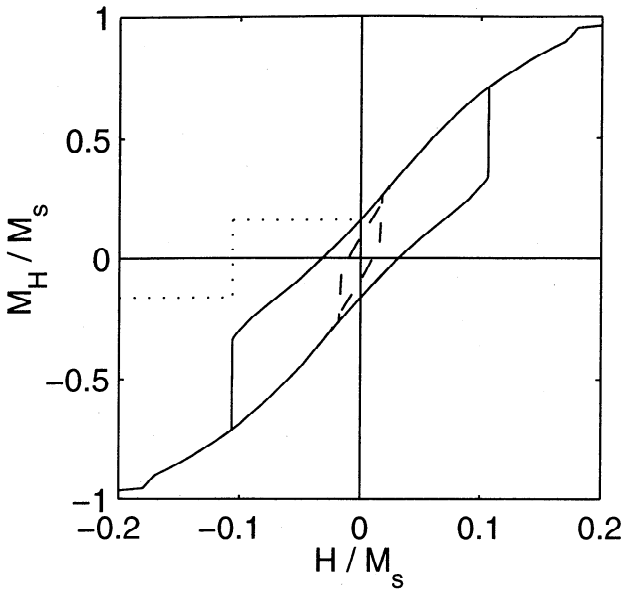

Figure 2. Hysteresis loop for a triaxial cuboid with $L = 0.09\,\mu$m and $\mathbf{H} \parallel (1, 8, 4)$. The conventions are the same as in Figure 1, but the horizontal scale is larger. Compared to Figure 1, the roles of remanent states are reversed, with the saturation remanent state having moment along the shortest axis. The long axis state is not accessible by a minor loop, but for completeness, we have calculated the magnetization curves for it (dashed curves).

branch or there was a different kind of singularity. Thus there is a greater uncertainty in some of the hysteresis parameters (particularly H_{cr}) for the $(1, 8, 4)$ direction.

4. Results

Newell and Merrill [this issue] found two basic kinds of state for all magnetic fields and grain sizes. The generalized SD state (also known as the flower state [*Schabes and Bertram*, 1988]) has zero curl in the magnetization, while the curling (vortex) state has nonzero curl. The transition between the SD and curling state is generalized curling mode nucleation [*Newell and Merrill*, 1998], which we will refer to as nucleation. The critical size at which nucleation occurs in zero field was called $L_{\mathrm{SD}}^{\mathrm{rem}}$ by *Newell and Merrill* [1999], who also showed that $L_{\mathrm{SD}}^{\mathrm{rem}}$ could be calculated analytically for spheroids. The analytical prediction works fairly well for small cubes [*Newell and Merrill*, this issue].

There are curling states with moments along each of the three axes. *Newell and Merrill* [this issue] called them long, intermediate, and short axis curling states. The long and short axis states are illustrated in Figure 3. The long axis state has a much larger moment, with $M > 0.95M_s$ compared to $M < 0.4M_s$ for the short axis state. The moment of the short axis state is also more concentrated about a central axis. Although the total moment is in the y direction, most of the internal magnetization is in the xz plane. This magnetization does not contribute to the moment because opposing magnetization vectors cancel out. Having more of the magnetization parallel to the long axis lowers the magnetostatic energy.

We will look at the size dependence of M_{rs}, H_c, H_{cr}, and χ_0 separately and then construct a Day plot. The size dependence of remanence is determined by three factors: the size dependence of the moment in each remanent state, the choice of remanent state, and the angle of the moment with respect to the field. We first focus on the magnitude of the moment in section 4.1 and then in section 4.2 determine the contribution of each state to the remanence.

4.1. Size Dependence of Moments

In Figure 4 we plot the size dependence of the moment for each state. The cube has three equivalent states (one for each axis), each of which nucleates at $L_{\mathrm{SD}}^{\mathrm{rem}} = 0.061\,\mu$m and changes continuously at all sizes. By contrast, the triaxial cuboid has a different curve for each axis. The only SD state has its moment along the long axis; this changes to a curling state at $L_{\mathrm{SD}}^{\mathrm{rem}} = 0.08\,\mu$m, and the curling state becomes unstable at $0.104\,\mu$m. The intermediate and short axis curling states are stable in large grains, but the intermediate axis state is unstable below $0.062\,\mu$m, and the short axis state is unstable below $0.067\,\mu$m. The moments of the long axis states increase with increasing grain size (more slowly after nucleation), but those of the other curling states decrease.

For comparison, we include calculations by *Fabian et al.* [1996] for similar grain shapes (a cube and a cuboid with square cross section and aspect ratio 1.52) and nonzero magnetocrystalline anisotropy. They set the anisotropy constant K_1 equal to the value for magnetite and oriented the $\langle 100 \rangle$ hard axes perpendicular to the surfaces. *Fabian et al.* [1996] did not simulate hysteresis or grain growth. Instead, for each of two initial guesses (called SD and vortex) they searched for a solution in zero field only. They obtained three kinds of states. Two of them, the flower and vortex states, correspond to our SD and short axis curling states. The third, which they called the double vortex state, has the magnetization in the center pointing along a $\langle 111 \rangle$ easy axis (similar to the diagonal vortex state of *Newell et al.* [1993a]).

Since $|K_1|/\mu_0 M_s^2 \approx 0.04$ in magnetite, a dimensional analysis would imply that magnetocrystalline anisotropy can be neglected to first order. However, under some circumstances the other energy terms may nearly cancel out. In the SD size range the moments with and without magnetocrystalline anisotropy do not differ significantly. Above $\approx 0.08\,\mu$m it would seem that magnetocrystalline anisotropy makes a big difference. The flower state remains nearly saturated up to $\approx 0.14\,\mu$m in the cube and $0.25\,\mu$m in the elongated grain. The moments at these sizes are as much as 32 times those of our curling states. For both grain shapes, when the flower state becomes unstable it is replaced by

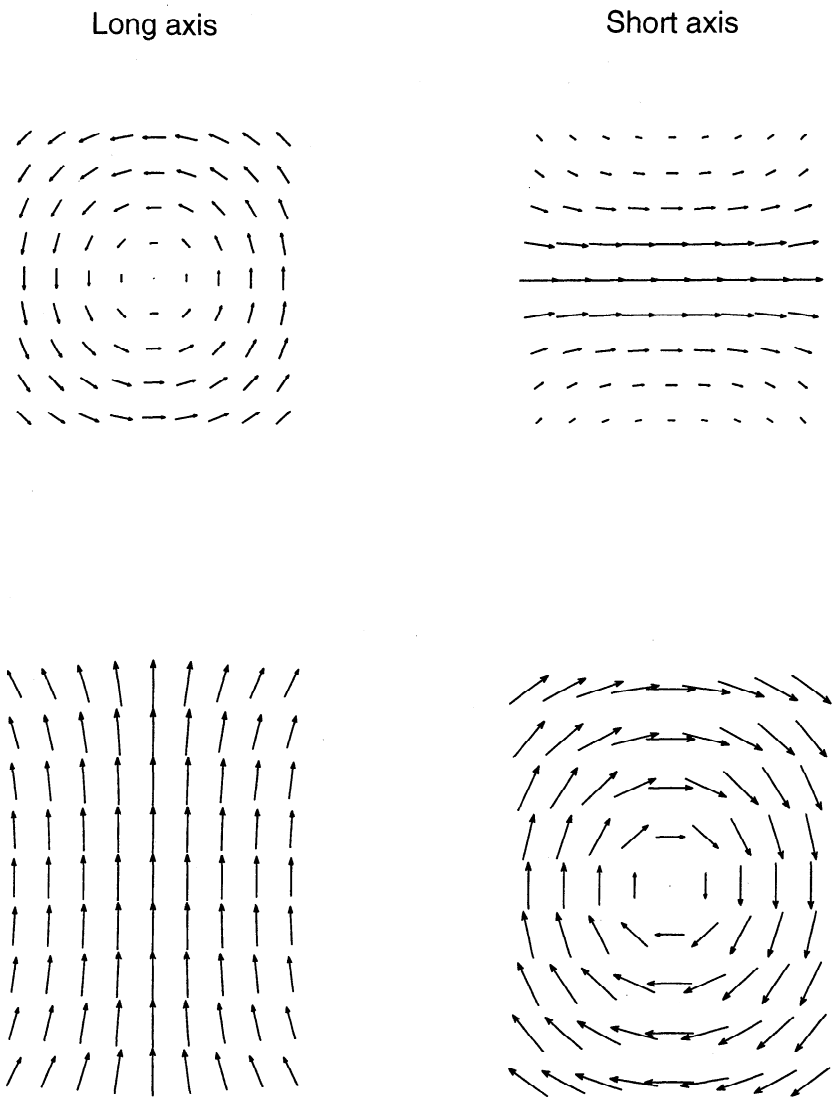

Figure 3. The magnetization in the long and short axis curling states for $L = 0.09\,\mu$m. The vectors represent the in-plane component of magnetization for cross sections through the central top (yz) and bottom (xz) planes. The long axis state has moment in the x direction and the short axis state has moment in the y direction. Since $|\mathbf{M}| = M_s$, a small vector indicates a large component perpendicular to the plane. All the points are calculated for the 9^3 discretization.

the double vortex state, which also has a much larger moment than the curling states. However, their solutions for the vortex initial guess look similar to our short axis curling state and have similar moments. Without hysteresis simulations we do not know which state is the saturation remanent state.

The flower states with large moments are probably unstable. In our model, nucleation occurs at $L_{\mathrm{SD}}^{\mathrm{rem}} = 0.061\,\mu$m in the cube and $0.08\,\mu$m in the triaxial cuboid. These sizes are close to the predictions of nucleation theory for spheroids [*Newell and Merrill*, this issue]. If the long axis is parallel to a magnetocrystalline easy axis, $L_{\mathrm{SD}}^{\mathrm{rem}}$ is larger, although the effect is small in magnetite [*Newell and Merrill*, 1999]. In the calculations of *Fabian et al.* [1996] the long axis is parallel to a hard axis, so $L_{\mathrm{SD}}^{\mathrm{rem}}$ should be even smaller than it is for $K_1 = 0$.

As *Newell and Merrill* [1998] showed, it is easy to miss the nucleation point and to continue on an unstable branch. Indeed, in hysteresis simulations, there is a systematic bias in the initial search direction, and unless a random perturbation is added, the search tends to jump past the point where the SD and curling states meet. The method of *Fabian et al.* [1996], with a SD initial guess, is like starting at saturation and quenching the field. Such a procedure will have an even greater bias in the search.

In section 4.2 we will describe how the changes in state affect the hysteresis parameters.

4.2. Saturation Remanence

The size dependence of M_{rs}/M_s is shown in Figure 5. If the magnetization were uniform, M_{rs}/M_s would

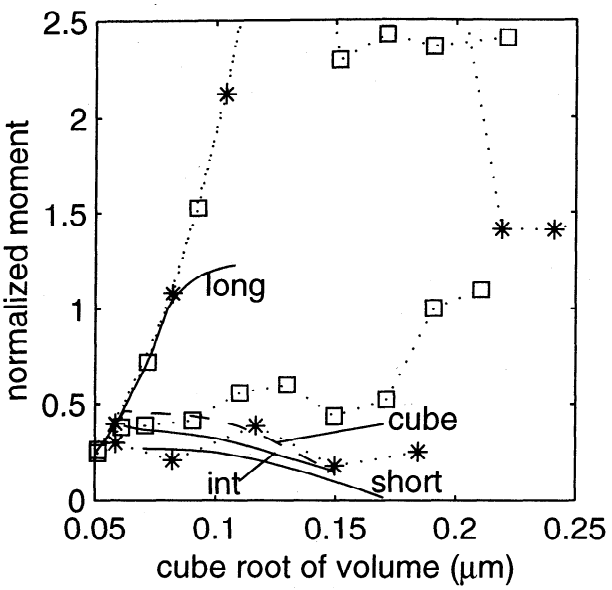

Figure 4. Size dependence of the moments of the remanent states, normalized to the moment of the long axis state at $L = L_{SD}^{rem}$. Solid curves represent the states in the triaxial cuboid with moments along the long, intermediate and short axes. The dashed curve is for the cube. Also shown are calculations of *Fabian et al.* [1996] for a cube (squares) and cuboid with aspect ratio 1.52 (asterisks). There are two sequences of states for each shape; each sequence is connected by dotted curves.

be $8/\sqrt{8^2+4^2+1^2} = 8/9$ for a field in the $(8,4,1)$ direction and $1/9$ for a field in the $(1,8,4)$ direction. Up to $L = L_{SD}^{rem}$, the remanent state is SD, and the remanence is within 5% of these values, indicating near saturation. When the grain size crosses L_{SD}^{rem}, M_{rs} changes continuously, but there is a sudden change in the slope of the magnetization curve [*Newell and Merrill*, this issue]. Between L_{SD}^{rem} and $0.09\,\mu$m, the remanent state for both field directions is the long axis curling state, and the ratio between the remanences remains 8 : 1.

The largest changes in remanence occur when the the short axis curling state becomes the saturation remanent state. The size at which this occurs depends on the direction of the field and is smaller for $\mathbf{H} \parallel (1,8,4)$. The moment decreases by a factor of ≈ 4.5 across the jump. However, the moment also rotates by 90°, and this can increase or decrease the remanence depending on the angle of the field. The net result is that for $\mathbf{H} \parallel (8,4,1)$, M_{rs}/M_s drops by a factor of 50, while for $\mathbf{H} \parallel (1,8,4)$, it increases by a small amount.

In the SD size range and up to $0.09\,\mu$m the remanent state always has its moment parallel to the long axis. Above $0.104\,\mu$m the moment is always parallel to the short axis. For these size ranges we can calculate the average remanence for a sample with randomly oriented grains. As for SD grains with uniaxial anisotropy [*Stoner and Wohlfarth*, 1947], we simply multiply the total moment by 0.5. The results are shown as dot-dashed curves in Figure 5. Between 0.09 and $0.104\,\mu$m the average M_{rs}/M_s drops from 0.4 to 0.06. Since the usual criterion for MD remanence is $M_{rs}/M_s < 0.05$, the remanence drops almost all the way across the PSD range.

The average remanence for a cube is also easily calculated. The moment is always perpendicular to a face, and all the faces are equivalent. Thus we can treat the remanence as we do for an SD grain with ⟨100⟩ easy axes and multiply the moment by 0.831. The remanence curve is continuous (Figure 5), and the critical size for nucleation is lower ($L_{SD}^{rem} = 0.061\,\mu$m). In the SD size range the cube has a larger remanence because there are six equivalent remanent states instead of two. This decreases the average angle of the moment with respect to the field. After nucleation occurs, the remanence dips briefly below that of the triaxial cuboid. However, for $L \geq 0.104\,\mu$m the remanence is larger again. If we compare the moments of remanent states in a cube and triaxial cuboid with the same volume, the moment of the cube is smaller than that of the long axis state but larger than that of the short axis state.

Thus, aside from a small size range above $0.061\,\mu$m the calculated remanence is larger in the cube than the more elongated body. However, thermal fluctuations will reduce the remanence near the SP/SD transition. The volume at this transition is particularly large in the cube because it has low-energy barriers between states.

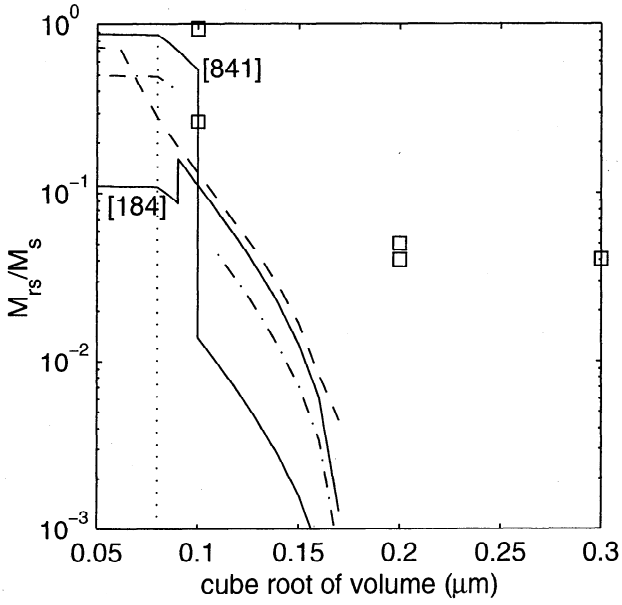

Figure 5. Size dependence of M_{rs}/M_s. The solid curves are the single grain curves for the cuboid with the field directions indicated beside them. For $L \leq 0.09\,\mu$m and $L \geq 0.104\,\mu$m the average for randomly oriented cuboids is plotted (dot-dashed curves). The dashed curve is the average for randomly oriented cubes (zero magnetocrystalline anisotropy). The squares are calculations of *Williams and Dunlop* [1995] for magnetite cubes with magnetocrystalline anisotropy included. The vertical dotted line indicates the critical size L_{SD}^{rem}.

The SD size range in the cube is almost nonexistent [*Newell and Merrill*, 1999]. Also, the trend of decreasing remanence with increasing aspect ratio will eventually reverse as the upper limit for SD remanence (L_{SD}^{rem}) increases. For small aspect ratios, L_{SD}^{rem} changes little, but near an aspect ratio of 5 in magnetite it rapidly increases to infinity.

In Figure 5 we include calculations by *Williams and Dunlop* [1995] for a magnetocrystalline anisotropy ($K_1 < 0$) with [100] hard axes perpendicular to the faces of the cube. We cannot determine M_{rs} from the moments of *Fabian et al.* [1996] because they did not give the directions and we do not know which state is the saturation remanent state. For some grain sizes, *Williams and Dunlop* [1995] calculated hysteresis curves for two field directions, the ⟨111⟩ easy and ⟨100⟩ hard directions. These two directions should give the maximum and minimum values of M_{rs}/M_s. The difference was relatively small, so *Williams and Dunlop* [1995] concluded that magnetocrystalline anisotropy is not important. However, if we compare their calculations with ours for the isotropic cube, we come to the opposite conclusion. Even near the SD size range, magnetocrystalline anisotropy increases the remanence. The size dependence is also much weaker. If their results and ours are both correct, magnetocrystalline anisotropy increases the remanence by orders of magnitude in larger cubes.

It is not clear whether magnetocrystalline anisotropy is equally important in a more elongated grain. If the higher-moment states in Figure 3 are real, the moment increases rapidly with grain size. If not, the remanent states are vortex states and magnetocrystalline anisotropy makes little difference.

4.3. Coercivity and Coercivity of Remanence

Newell and Merrill [1999] pointed out that the first change in coercivity of remanence should occur at a critical size L_{SD}^{coerc} where the mode of nucleation changes from nearly uniform rotation to curling. For $L < L_{SD}^{coerc}$, H_{cr} should be close to its SD value. In larger grains the change of mode should decrease H_{cr}. Unlike the remanence critical size L_{SD}^{rem}, L_{SD}^{coerc} depends on the direction of the field. Nucleation may also reduce the coercivity, but it depends on the angle of the field. In Figure 1 the first jump crosses $M = 0$, so $H_c = H_{cr}$. In Figure 2 the magnetization changes sign well before a jump occurs. Thus we can expect nucleation to reduce H_c when $\mathbf{H} \parallel (8,4,1)$, but it has no immediate effect when $\mathbf{H} \parallel (1,8,4)$.

In Figure 6 we plot H_c and H_{cr} as a function of grain size. As we argued above, when $\mathbf{H} \parallel (8,4,1)$, both parameters drop suddenly at $L_{SD}^{coerc} \approx 0.074\,\mu$m. When $\mathbf{H} \parallel (1,8,4)$, there is a jump in H_{cr} but not H_c at $L_{SD}^{coerc} \approx 0.08\,\mu$m.

In section 4.2 we showed that the largest jumps in M_{rs}/M_s occur when the saturation remanent state changes from the long axis curling state to the short axis curling state. As Figures 1 and 2 demonstrate, in larger grains the short axis state is much more stable than the long axis state. Thus when the jump occurs, there is a large increase in H_{cr}. There is also a small increase in H_c.

For $\mathbf{H} \parallel (8,4,1)$ the coercivity is very small and decreasing through $L = 0.1\,\mu$m. If our resolution were greater, we would see it approach zero at $L = 0.104\,\mu$m. This can be seen by the following argument. In Figure 1 the long axis state jumps to a short axis state. It has two choices, corresponding to positive and negative remanence, but the latter has a lower energy in a negative field. Thus the magnetization changes sign when the

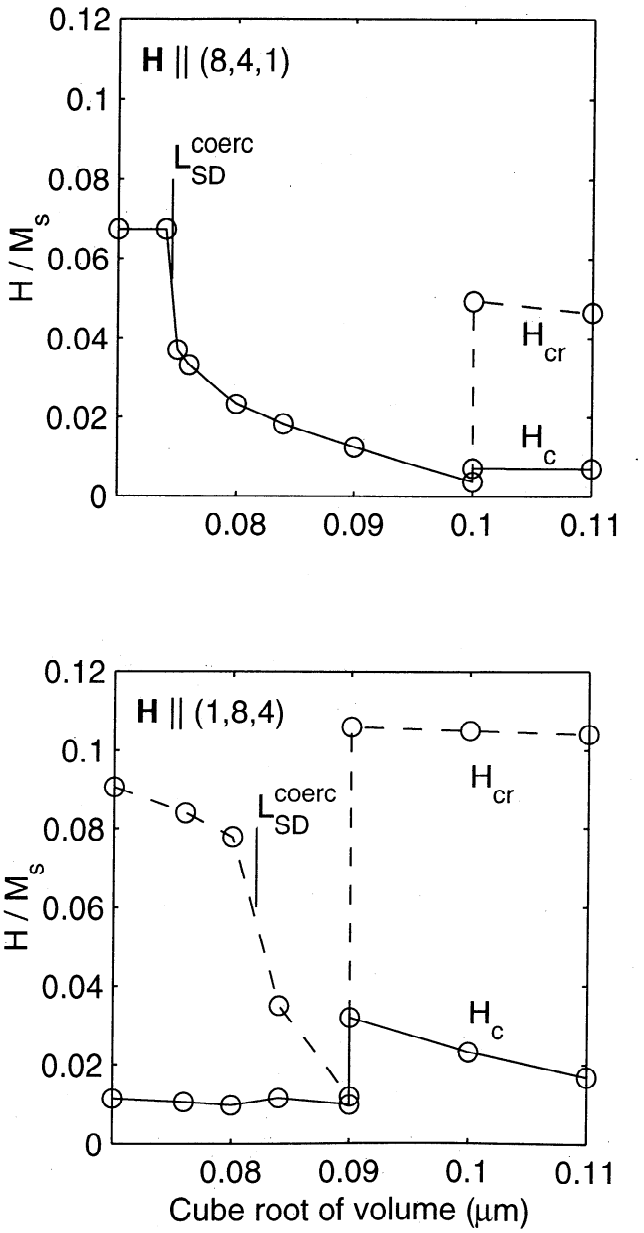

Figure 6. The size dependence of the single-particle coercivity(solid curves) and coercivity of remanence (dashed curves) for the triaxial cuboid. Significant changes occur at the critical sizes L_{SD}^{coerc} and L_{2D}.

jump occurs, and as the grain size approaches $0.104\,\mu$m the coercivity approaches zero. In larger grains the jump occurs in a positive field, and the magnetization chooses the branch with positive remanence because it now has the lowest energy [*Newell and Merrill*, this issue, Figure 11]. Thus H_c and H_{cr} suddenly increase. By contrast, if the field is in the $(1,8,4)$ direction, no such effect is seen because the jump from long axis state to short axis state always occurs in a positive field.

Samples of interest to paleomagnetists have random grain orientations, and they also have a wide range of grain sizes. Unfortunately, it is difficult to calculate average values of H_c and H_{cr} even for SD grains [*Stoner and Wohlfarth*, 1947]. However, on the basis of the curves in Figure 6 we expect that if the coercivities are averaged over random orientations and a broad range of sizes, H_c will decrease monotonically and H_{cr} will change little. This is consistent with the observations of *Heider et al.* [1996].

4.4. Initial Susceptibility

To understand the size dependence of χ_0, it helps to look at how the slope of the magnetization curve, $\chi(H) = dM_H/dH$, depends on the field. In Figure 7 we plot $\chi(H)$ for the magnetization curves in Figure 1; $\chi(H)$ is small in large fields. When nucleation occurs near $H = 0.04M_s$, the magnetization changes continuously, but there is a sudden increase in $\chi(H)$ (see *Newell and Merrill* [this issue] for details). At $H = -0.013M_s$, there is a jump from the long axis state to the short axis state. As the field approaches the jump, $\chi(H)$ approaches infinity. It returns to a finite value after the jump, but quickly approaches infinity again as the second jump nears.

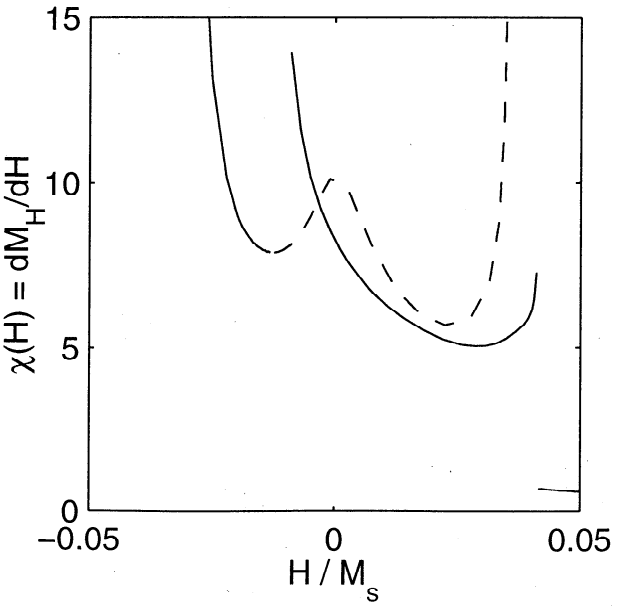

Figure 7. Field-dependent susceptibility $\chi(H)$ for $L = 0.09\,\mu$m and $\mathbf{H} \parallel (8,4,1)$ (the hysteresis loop is shown in Figure 1). The solid curves are for the main loop, and the dashed curve is for the minor branch.

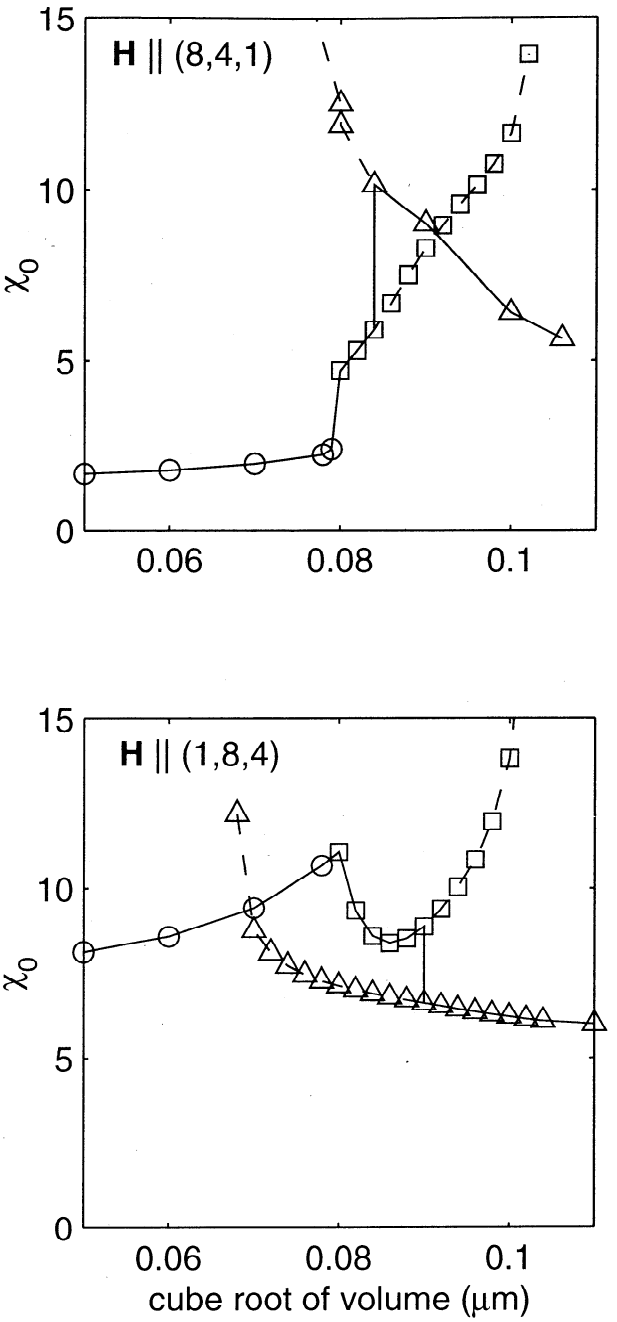

Figure 8. The size dependence of χ_0. Circles indicate the SD state, squares indicate the long axis curling state, and triangles indicate the short axis curling state. The solid curve is for the AF demagnetized state, while the dashed curves continue χ_0 for each state beyond the size range for which it is the AF demagnetized state.

On the minor branch, there is a cusp-like maximum in $\chi(H)$ at $H = 0$. The long axis curling state does not have this feature. As we will discuss in a future article, this is an indication that the magnetization changes by a different mechanism in the two states.

The size dependence of χ_0 is shown in Figure 8. Because of nucleation, there is a jump in χ_0 at $L_{\mathrm{SD}}^{\mathrm{rem}}$, although for $\mathbf{H} \parallel (1,8,4)$ the jump is too small to resolve clearly. (*Heider et al.* [1996] obtained a similar result but did not comment on it. On the basis of our

analysis the upward trends in their plot probably indicate the approach of nucleation.) The next jump occurs when the AF demagnetized state switches from the long axis curling state to the short axis curling state. The switch occurs when a minor branch first appears in the hysteresis. For $\mathbf{H} \parallel (8,4,1)$ the AF demagnetized state changes sooner than the saturation remanent state ($0.084\,\mu$m compared to $0.104\,\mu$m). When $\mathbf{H} \parallel (1,8,4)$, both kinds of remanence change at the same size.

Within each continuous segment in Figure 8, χ_0 varies a lot. To provide context, we extend the χ_0 curve for each state to sizes for which it is not the AF demagnetized state (dashed curves). As L approaches $0.104\,\mu$m, the size at which the long axis state becomes unstable, its susceptibility approaches infinity. The same is true of the short axis state as L approaches $0.067\,\mu$m.

Overall, the size dependence of χ_0 is far from simple. Instead of being a single smooth (or even monotonic) trend, it can increase or decrease. Jumps occur when the AF demagnetized state switches from the SD to the long axis curling state and from that to the short axis curling state. In real samples, these changes will be smeared out by random grain orientations and size distributions, and we can expect a weak size dependence. Since we did not include magnetocrystalline or magnetoelastic anisotropy, our calculations are probably upper bounds for the real susceptibility.

4.5. Day Plot

Finally, in Figure 9 we show how the position on a *Day et al.* [1977] plot changes with grain size. Looking at this plot, we must keep in mind that the parameters are for single grains, not collections of randomly oriented grains. Depending on the angle of the field, a single SD grain can have values of M_{rs}/M_s between 0 and 1 and H_{cr}/H_c between 0 and infinity. The limiting SD values for $\mathbf{H} \parallel (8,4,1)$ are $M_{rs}/M_s = 8/9$ and $H_{cr}/H_c = 1$, while those for $\mathbf{H} \parallel (1,8,4)$ are $M_{rs}/M_s = 1/9$ and $H_{cr}/H_c \approx 8$.

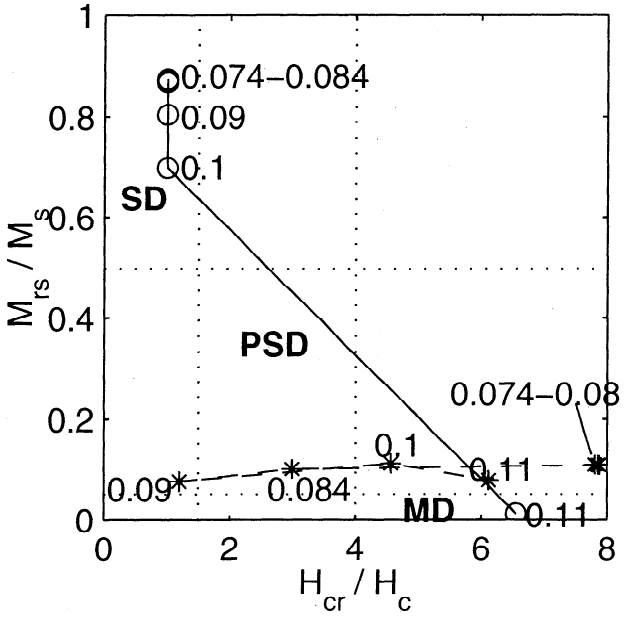

Figure 9. The progress of single grain hysteresis parameters on the Day diagram with increasing grain size. The circles indicate $\mathbf{H} \parallel (8,4,1)$, and the asterisks indicate $\mathbf{H} \parallel (1,8,4)$. The grain sizes in microns are indicated beside each point. The dotted curves are the boundaries between the SD, PSD, and MD regions, as defined by *Day et al.* [1977].

When the field is in the $(8,4,1)$ direction, M_{rs} starts decreasing at $L_{\mathrm{SD}}^{\mathrm{rem}} = 0.08\,\mu$m. H_c and H_{cr} start to decrease at $L_{\mathrm{SD}}^{\mathrm{coerc}} = 0.074\,\mu$m, but H_{cr}/H_c remains equal to 1 until the transition to the short axis remanent state at $0.104\,\mu$m. At this size the hysteresis parameters jump right across the PSD region and into the MD region.

When the field is in the $(1,8,4)$ direction, it is H_{cr}/H_c that changes rapidly above the SD size range (most of the change is in H_{cr}). Then, at $0.09\,\mu$m the short axis state takes over, and both M_{rs}/M_s and H_{cr}/H_c increase. Subsequently, the points move toward the MD region. By $L = 0.11\,\mu$m both field directions are in the same part of the Day plot, but the hysteresis properties still depend strongly on field direction.

Since there is a large jump in all the hysteresis parameters between $L = 0.09\,\mu$m and $L = 0.104\,\mu$m, it is probably not possible to interpret position on a Day plot in terms of a single characteristic grain size. As in the model of *Tauxe et al.* [1996], other measures of the grain size distribution may be as important as the mean grain size. *Tauxe et al.* [1996] also found that the main loop can be normal, wasp-waisted, or potbellied depending on the distribution of sizes. A similar effect can be expected if we mix the hysteresis curves for the grains in the SD and small PSD range. Indeed, as Figure 1 shows, a single grain can be wasp-waisted. In this case, there is a mixture of states with different stabilities rather than a mixture of grains.

5. Conclusions

We have shown that transitions between magnetic states, ignored in MD theories, have a major effect on hysteresis and remanence. The two main transitions are nucleation (uniform rotation or curling) and the jump from the long axis curling state to the short axis curling state. Curling mode nucleation is associated with two critical sizes [*Newell and Merrill*, 1999]. At $L_{\mathrm{SD}}^{\mathrm{coerc}}$, nucleation first appears in the hysteresis loop and decreases H_c and H_{cr}. At $L_{\mathrm{SD}}^{\mathrm{rem}}$, nucleation occurs in zero field, lowering M_{rs} and increasing χ_0.

We calculated the saturation remanence for a cube and a triaxial ($X = 1.5Y = 1.4Z$) cuboid. The cube is the most commonly modeled shape, but it is atypical in some respects. First, all the remanent states for a given grain size are equivalent, and its remanence changes continuously with size. The only event is a change in slope at $L_{\mathrm{SD}}^{\mathrm{rem}}$. By contrast, an elongated body has three curling states with unequal moments, the smallest moment being along the shortest axis. In elongated grains, there are two changes in remanence:

nucleation at L_{SD}^{rem} and then a jump from the long axis curling state to the short axis curling state. The latter change in remanence is large and should increase as the aspect ratio increases. The other difference is that the cube generally has a larger remanence than more elongated grains. At larger grain sizes this is because the curling state in the cube has a larger moment than the short axis curling state.

All the hysteresis parameters of the cuboid are affected when the remanent state switches from the long axis curling state to the short axis curling state. H_{cr} decreases before the switch, then rebounds to SD-like values. H_c also has a much smaller rebound, so H_{cr}/H_c jumps to the MD range. The average M_{rs}/M_s for randomly oriented grains drops from 0.4 when $L = 0.09\,\mu$m to 0.06 when $L = 0.104\,\mu$m. There is even a jump in χ_0 when the AF demagnetized state changes.

We can now return to the questions we asked at the beginning. Can the mean grain size be inferred from the Day plot or by some combination of hysteresis parameters? Perhaps it can be if the particles are cubic with a weak magnetocrystalline anisotropy, because then the remanence changes continuously. If the grains are elongated, our calculations imply that a grain size would be difficult to deduce, at least in grains near the SD size range ($L \leq 0.25\,\mu$m in magnetite). In the triaxial grain, χ_0 and H_{cr} fluctuate rapidly and show no systematic dependence on grain size. Over a negligible grain size interval the average remanence jumps almost all the way across the usual PSD range. This jump effectively divides grain sizes into SD and MD, so any remanences in the PSD range are determined by the proportion of SD and MD grains. The coercivity is the closest to having a smooth and monotonic size dependence.

The reader may well question the realism of our model results. The remanence drops very rapidly, reaching MD values by $0.11\,\mu$m, whereas such remanences are measured in much larger synthetic samples. However, real samples have a wide range of grain sizes. When the nominal size is SD, contributions from SP and PSD grains lower the remanence. When the nominal size is above the SD size range, smaller grains will increase the average remanence. Remanence calculations that take the grain size distribution into account raise some difficult questions that we will leave to a future article.

Perhaps in larger grains there is a simple size dependence of magnetic parameters. However, even if there is, *Tauxe et al.* [1996] showed that it can be mimicked by an SP/SD mixture. Distinguishing these mixtures from larger grains may require temperature-dependent measurements. It will also require better information on the size dependence of magnetic properties. Experimentally, we need better control on grain size and shape, using techniques such as electron beam lithography [*King et al.*, 1996] However, even if we have accurate information on size dependence, to apply it to natural samples we will still need to include grain size explicitly.

Acknowledgments.
This research was supported by NSF grants EAR 9614138 and EAR 9814396. We would like to thank Jeff Gee, David Dunlop, and Ted Evans for commenting on the manuscript.

References

Berkov, D. V., K. Ramstöck, and A. Hubert, Solving micromagnetic problems: Towards an optimal numerical method, *Phys. Stat. Sol. A*, *137*, 207–225, 1993.

Brown, W. F., Jr., *Micromagnetics*, 143 pp., Interscience, New York, 1963, (Reprinted by Krieger, New York, 1978.)

Day, R., M. Fuller, and V. A. Schmidt, Hysteresis properties of titanomagnetites: grain-size and compositional dependence, *Phys. Earth Planet. Inter.*, *13*, 260–267, 1977.

Dunlop, D. J., and O. Özdemir, *Rock Magnetism: Fundamentals and Frontiers*, 573 pp., Cambridge Univ. Press, New York, 1997.

Enkin, R. J., Micromagnetic study of pseudo-single-domain structure - Applications to rock magnetism, Ph.D. thesis, 131 pp., Univ. of Toronto, Toronto, Ont., 1986.

Fabian, K., A. Kirchner, W. Williams, F. Heider, A. Hubert, and T. Leibl, Three-dimensional micromagnetic calculations for magnetite using FFT, *Geophys. J. Int.*, *124*, 89–104, 1996.

Gee, J., and D. V. Kent, Magnetic hysteresis in young mid-ocean ridge basalts: Dominant cubic anisotropy?, *Geophys. Res. Lett.*, *22*, 551–554, 1995.

Halgedahl, S. L., Bitter patterns versus hysteresis behavior in small single particles of hematite, *J. Geophys. Res.*, *100*, 353–364, 1995.

Heider, F., D. J. Dunlop, and N. Sugiura, Magnetic properties of hydrothermally recrystallized magnetite crystals, *Science*, *236*, 1287–1290, 1987.

Heider, F., A. Zitzelsberger, and K. Fabian, Magnetic susceptibility and remanent coercive force in grown magnetite crystals from $0.1\,\mu$m to 6mm, *Phys. Earth Planet. Inter.*, *93*, 239–256, 1996.

Hubert, A., and R. Schäfer, *Magnetic Domains: The Analysis of Microstructures*, Springer-Verlag, New York, 1998.

Iooss, G., and D. D. Joseph, *Elementary Stability and Bifurcation Theory*, 2nd ed., 324 pp., Springer-Verlag, New York, 1990.

Jackson, M., Diagenetic sources of stable remanence in remagnetized Paleozoic cratonic carbonates: A rock magnetic study, *J. Geophys. Res.*, *95*, 2753–2761, 1990.

King, J. G., W. Williams, C. D. W. Wilkinson, S. McVitie, and J. N. Chapman, Magnetic properties of magnetite arrays produced by the method of electron beam lithography, *Geophys. Res. Lett.*, *23*, 2847–2850, 1996.

Néel, L., Some theoretical aspects of rock magnetism, *Adv. Phys.*, *4*, 191–243, 1955.

Newell, A. J., Theoretical calculations of magnetic hysteresis and critical sizes for transitions between single-domain and multi-domain properties in titanomagnetites, Ph.D. thesis, 188 pp., Univ. of Wash., Seattle, 1997.

Newell, A. J., and R. T. Merrill, The curling nucleation mode in a ferromagnetic cube, *J. Appl. Phys.*, *84*, 4394–4402, 1998.

Newell, A. J., and R. T. Merrill, Single-domain critical sizes for coercivity and remanence, *J. Geophys. Res.*, *104*, 617–628, 1999.

Newell, A. J., and R. T. Merrill, Nucleation and stability of remanent states, *J. Geophys. Res.*, this issue.

Newell, A. J., D. J. Dunlop, and W. Williams, A two-dimensional micromagnetic model of magnetizations and fields in magnetite, *J. Geophys. Res.*, *98*, 9533–9550, 1993a.

Newell, A. J., W. Williams, and D. J. Dunlop, A generalization of the demagnetizing tensor for nonuniform magnetization, *J. Geophys. Res.*, *98*, 9551–9556, 1993b.

Schabes, M. E., and H. N. Bertram, Magnetization processes in ferromagnetic cubes, *J. Appl. Phys.*, *64*, 1347–1357, 1988.

Stacey, F. D., The physical theory of rock magnetism, *Adv. Phys.*, *12*, 45–133, 1963.

Stoner, E. C., and E. P. Wohlfarth, A mechanism of magnetic hysteresis in heterogeneous alloys, *Philos. Trans. R. Soc. London Ser. A*, *240*, 599–642, 1947.

Suk, D., and S. Halgedahl, Hysteresis properties of magnetic spherules and whole rock specimens from some paleozoic platform carbonate rocks, *J. Geophys. Res.*, *101*, 25,053–25,075, 1996.

Tauxe, L., T. A. T. Mullender, and T. Pick, Potbellies, wasp-waists, and superparamagnetism in magnetic hysteresis, *J. Geophys. Res.*, *101*, 571–583, 1996.

Thompson, R., and F. Oldfield, *Environmental Magnetism*, 227 pp., Allen and Unwin, Winchester, Mass., 1986.

Verosub, K. L., and A. P. Roberts, Environmental magnetism: Past, present, and future, *J. Geophys. Res.*, *100*, 2175–2192, 1995.

Williams, W., and D. J. Dunlop, Three-dimensional micromagnetic modelling of ferromagnetic domain structure, *Nature*, *337*, 634–637, 1989.

Williams, W., and D. J. Dunlop, Simulation of magnetic hysteresis in pseudo-single-domain grains of magnetite, *J. Geophys. Res.*, *100*, 3859–3871, 1995.

R. T. Merrill, Geophysics Program, Box 351650, University of Washington, Seattle, WA 98195-1650. (ron@geophys.washington.edu)

A. J. Newell, Geological Sciences Department, University of California, Santa Barbara, CA 93106-9630. (newell@geol.ucsb.edu)

(Received August 2, 1999; revised February 21, 2000; accepted April 5, 2000.)